

Thin Films of Block Copolymer–Homopolymer Blends with a Continuously Tunable Density of Spherical Microdomains

John M. Papalia,^{†,‡} Andrew P. Marencic,[†]
Douglas H. Adamson,^{‡,‡} Paul M. Chaikin,^{‡,§} and
Richard A. Register^{*,†,‡}

[†]Department of Chemical and Biological Engineering, [‡]Princeton Institute for the Science and Technology of Materials, Princeton University, Princeton, New Jersey 08544, [‡]Department of Chemistry and Institute of Materials Science, University of Connecticut, Storrs, Connecticut, 06269, and [§]Department of Physics, New York University, New York, New York 10003

Received June 30, 2010

Revised Manuscript Received July 30, 2010

Block copolymers have been extensively studied for their ability to self-assemble into microdomain morphologies such as spheres, cylinders, and lamellae, with typical periodicities of 20–100 nm.^{1,2} Similar structures form when block copolymers are deposited as thin films on substrates;^{3,4} for example, very asymmetric block copolymers form spheres (micelles) of the minority component in a matrix of the majority block. Films containing a single layer of spherical micelles have been used effectively as templates for the synthesis of dense ($\sim 10^{11}$ per cm^2), substrate-supported arrays of uniform-size “dots”. These dots can be formed from materials as diverse as metals (Au,^{5,6} W,⁷ CoPt alloy⁸), oxides (SiOx⁹), III–V semiconductors (GaAs¹⁰), and conducting polymers (polyaniline¹¹), where each dot replicates—in the material of choice—the shape and position of a micelle in the template. While much interest has focused on creating arrays with the highest possible density of dots, there are also applications where lower-density arrays are preferred, particularly when some minimum spacing between the features is needed to minimize interference between processes occurring at the individual dots. Examples include electron emitter tips for compact charging devices,¹² and catalyst particle arrays for nanowire growth in the vapor–liquid–solid process.¹³ In applications such as these, periodic order of the dots (or of the microdomains in the templating film) is not required. Instead, the desirable features of employing a block copolymer as a template in these contexts are that it ensures: (1) a uniform size of the dots, (2) a minimum spacing between the dots (set by the corona thicknesses of two adjacent micelles), and (3) a statistically uniform distribution of the dots on the micrometer scale and above (i.e., no micelle-rich or micelle-poor regions). This contrasts with simple deposition of nanoparticles from solution, where particle–particle contact and aggregation can easily occur. Here, we take advantage of the through-film structures of block copolymer thin films, and the behavior of block copolymer/homopolymer blends, to continuously tune the areal density of micelles all the way from zero up to values comparable to that for a monolayer of neat block copolymer; this is accomplished simply by control of the film thickness, all at a constant ratio (~ 1) of block copolymer to homopolymer.

Our approach is shown graphically in Figure 1. It relies crucially on the fact that the two dissimilar blocks in the copolymer have preferential interactions with the substrate and with the free surface, leading typically to complete wetting of each surface by one of the blocks. When the wetting block is the minority component, this results in the formation of a brush-like “wetting layer” at that interface; such wetting layers are shown schematically in Figure 1, for the case where the minority block (blue) wets both the substrate and the free surface.¹⁴ Since the block chemistry and length ratio can be varied over a wide range at the time of synthesis, block copolymers can be designed where the minority component wets both surfaces, either of the two, or neither. The approach we describe here requires that the minority component wet at least one of the two surfaces. In this case, the wetting layers, which have a combined thickness b , will constitute the entire film for film thicknesses t , when $t \leq b$; only for film thicknesses $t > b$ is there enough material to begin to form spherical microdomains.¹⁵ However, in neat block copolymers, where the chains have sufficient mobility to rearrange, the “extra” material (for $t > b$) typically goes to form micrometer-width “islands” (Figure 1a) with a thickness exceeding that of the wetting layers by an amount m , corresponding to a single layer of microdomains (see Figure 1b). As the film thickness is increased, the islands coalesce, such that the topology changes¹⁶ to a film which has a largely continuous layer of microdomains, perforated by “holes” — micrometer-width regions containing only the wetting layer. Since the islands/holes (collectively referred to as “terraces”) cover fractions of the film dictated by the amount of material deposited on the substrate (initial film thickness), the average areal density of the micelles can be controlled by film thickness—but it is highly nonuniform, since the film consists of regions of wetting layer only (bereft of micelles, left sides of parts a and b of Figure 1) and other regions which contain micelles at a density equal to that in a full monolayer (right side of parts a and b of Figure 1). To obtain a film with a uniform distribution of micelles on the micrometer scale and above, terracing must be suppressed; in this case, the film thickness will control the areal density, as shown schematically in Figure 1c. This direct connection between micelle areal density and film thickness is a consequence of the fact that the material’s composition is uniform on length scales much larger than the individual micelle—in other words, that the local ratio of red to blue in Figure 1c is constant regardless of film thickness—but that the wetting layers are of uniform thickness (b) when the film thickness exceeds the minimum required for micelles to form (t_0 in Figure 1c).

Terracing is driven by the fact that, for a given block copolymer, there is a strongly preferred microdomain size and spacing dictated principally by the balance between enthalpically unfavorable interactions involving dissimilar blocks (at the micelle core–corona boundary), tending toward a larger periodicity, and entropically unfavorable stretching of the blocks, tending toward a smaller periodicity.^{1,2} Stretching of the corona blocks can be mitigated by the addition of matrix homopolymer,¹⁷ as illustrated schematically in Figure 2. In the “dry brush” limit, which pertains when the molecular weight of the homopolymer is high, there is negligible penetration of the corona

*Corresponding author. E-mail: register@princeton.edu.

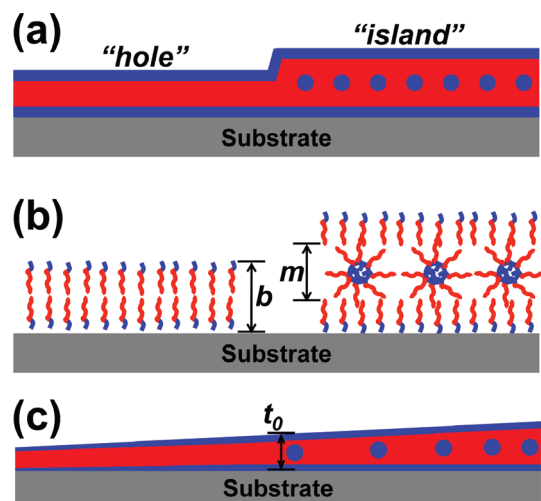


Figure 1. Representations of a diblock copolymer thin film and associated wetting layers; the majority block is shown in red and the minority block in blue, and the case where the minority component wets both surfaces is shown: (a) terraces ("islands" and "holes") that can form in a film of incommensurate thickness; (b) schematic arrangement of the chains corresponding to these terraces, with brush-like wetting layers of thickness b in the hole areas, and with a layer of micelles sandwiched between the wetting layers in the island areas, contributing a thickness increment m ; (c) a thickness gradient film, where terraces have been suppressed and a variable areal density of micelles has been achieved above a minimum film thickness, t_0 .

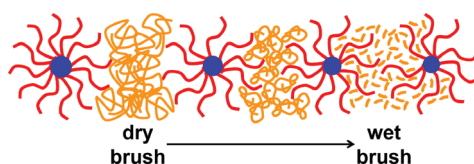


Figure 2. Representation of the penetration regimes in blends of micelle-forming block copolymer with homopolymer (shown in orange) having the same chemical composition as the micelle coronae but differing in molecular weight. In the "dry brush" limit (left), there is negligible penetration of the corona by homopolymer, while in the "wet brush" limit (right), the corona is swollen by the homopolymer, leading to stronger curvature and reduced micelle size.

blocks by the homopolymer; the homopolymer resides between micelles. If the homopolymer content is sufficiently large, it can completely screen the interactions between the coronae of neighboring micelles, thus eliminating the driving force both to form a periodic lattice of microdomains in bulk¹⁸ and to form terraces in thin films. As the homopolymer molecular weight is reduced, the homopolymer begins to penetrate the corona; in the "wet brush" limit of very low homopolymer molecular weight, the homopolymer is distributed throughout the corona, as would be the case for a simple solvent. The transition between "dry" and "wet" regimes is not sharp, but is expected to occur when the ratio of homopolymer to corona block molecular weights is approximately unity.¹⁹

Thickness-Gradient Films. For this work, we employed a polystyrene–polyisoprene diblock copolymer, PS/PI 62/11, with number-average molecular weights (M_n) of 62 and 11 kg/mol for the PS and PI blocks, respectively. This is the identical diblock used previously to fabricate fully dense arrays of both Au^{5,6} and GaAs¹⁰ dots, so its suitability as a template for pattern transfer (via removal of the PI block by ozonolysis, followed by transfer into the substrate via reactive ion etching) has already been demonstrated. The PI block is known to wet the native oxide on the Si wafer

substrate,¹⁴ as well as the free surface (PI has the lower surface tension²⁰), so a pair of wetting layers is formed,¹⁴ as shown in Figure 1. To suppress terracing, we blended PS/PI 62/11 with high loadings (50 or 60 wt %) of one of three homopolystyrenes of varying molecular weights ($M_n = 2.3, 45, \text{ or } 107 \text{ kg/mol}$); these molecular weights were chosen to span the wet brush, transition, and dry brush regimes, respectively.

To elucidate the relationship between micelle areal density and film thickness, we used a flow coater based on the design of Stafford et al.²¹ to create wafer-scale films with controllable thickness gradients. Since measurements of film thickness and micelle density can be made locally at various positions across the film, a single thickness-gradient film can yield the entire micelle density vs film thickness relationship for a given block copolymer-homopolymer blend, rather than spin-coating dozens of uniform-thickness films and measuring each individually. The thickness gradient idea is shown schematically in Figure 1c, where the thickness gradient will lead in turn to a gradient in micelle density (increasing with film thickness). Toluene solutions (5 wt % solids) were used to coat films with thicknesses ranging from 40 to 130 nm onto commercial Si wafers bearing the native oxide (see Supporting Information for details). Films were annealed at 165 °C under rough vacuum for 2 h to allow the structures to approach equilibrium, then cooled to room temperature under vacuum. The presence or absence of terraces was determined by optical microscopy (OM; Olympus BX60). Thickness profiles for each film were measured using microspot ellipsometry (10 $\mu\text{m} \times 30 \mu\text{m}$; Gaertner LS116S300), at locations on a rectangular grid. The substrate-supported films were then stained via the vapors of 0.5% aqueous OsO₄ and imaged with scanning electron microscopy (SEM; Philips/FEI XL30) using backscattered electron detection. Micelle areal density was determined by automated image analysis²² using a suitably chosen brightness threshold (see Supporting Information for details).

Film Structure. A thickness gradient film of neat PS/PI 62/11 was prepared for comparison, and was annealed at higher temperature (180 °C) for an extended period (7 days), under diffusion pump vacuum, to allow terracing to proceed as far as possible without incurring degradation of the polymer. This thickness gradient film showed an untterraced "band" surrounding $t = 69 \text{ nm}$, corresponding to a monolayer of spheres; holes were observed at $t = 66 \text{ nm}$, and islands (representing bilayers of spheres) at $t = 72 \text{ nm}$, so $m+b$ (the thickness of a monolayer) is $69 \text{ nm} (\pm 3 \text{ nm})$. In the monolayer region, the film showed a local hexagonal packing of the spheres. High-contrast SEM images of Au dots fabricated from this block copolymer template⁶ yielded a center-to-center spacing (hexagonal lattice parameter) $a = 38 \text{ nm}$, corresponding to an areal density of $800 \text{ micelles}/\mu\text{m}^2$, in good agreement with the $810 \text{ micelles}/\mu\text{m}^2$ measured on monolayer films of the neat OsO₄-stained block copolymer, using the same image analysis protocol employed for the thickness gradient films of the block copolymer-homopolymer blends. The thickness of a single layer of hexagonally packed microdomains in a stack of such layers (with ABA or ABC stacking, or a mixture of the two) is simply $(2/3)^{1/2}a$, so $m = 31 \text{ nm}$, and $b = 38 \text{ nm}$. The similarity between m and b is expected, since b corresponds to a pair of wetting layers for PS/PI.

Figure 3 shows a montage of SEM and OM images taken at various positions (film thicknesses) along three gradient films, each containing 50 wt % homopolymer of a different molecular weight; PI spheres appear bright in the SEM images due to the OsO₄ staining. The 50 wt %/2.3K film

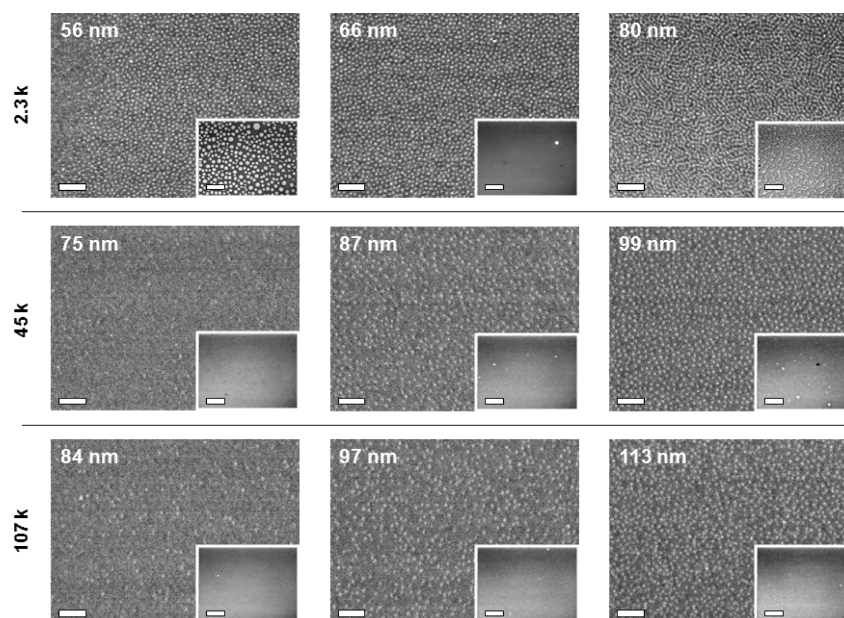


Figure 3. SEM and OM (inset) images taken at different positions (columns) on three different thickness-gradient films (rows), each with a homopolymer volume fraction $\phi = 0.494$. Film thickness increases from left to right; each row corresponds to a film containing a homopolymer of different molecular weight, as indicated along the left margin. Scale bars are 200 nm for the SEM images and 50 μm for the OM images.

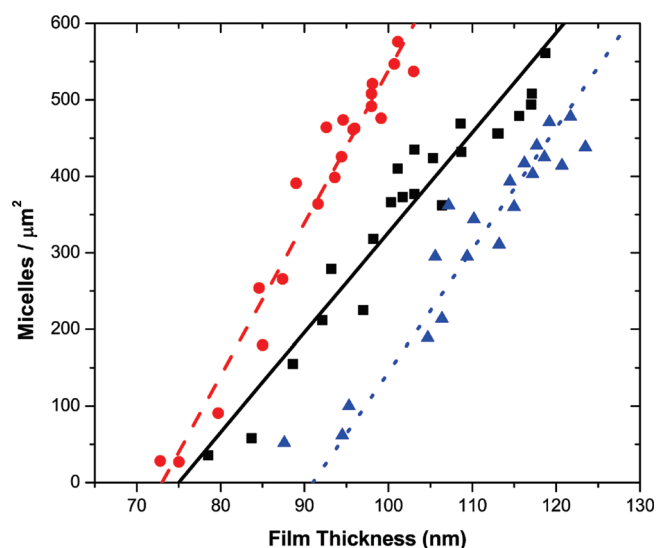


Figure 4. Measured micelle areal densities (symbols) for different film thicknesses in three diblock-homopolymer blends: 50 wt %/107K (black squares), 50 wt %/45K (red circles), and 60 wt %/45K (blue triangles). Corresponding model calculations are shown as lines: 50 wt %/107K (black, solid), 50 wt %/45K (red, dashed), and 60 wt %/45K (blue, dotted). For the 50 wt %/107K film, the model calculation uses brush thickness and micelle size parameters determined directly from the neat diblock copolymer; for the 50 wt %/45K and 60 wt %/45K films, these values are reduced slightly to account for partial interpenetration of the homopolymer into the brush layers and micelle coronae.

(top row of images) shows extensive terrace formation—the situation we wish to avoid. The $t = 56$ nm film shows mostly monolayer regions, with holes of wetting layer present, which are the bright features in the OM image (inset); the featureless left edge of the SEM image corresponds to such a hole. The $t = 80$ nm film is also mostly monolayer, with bilayer islands; since backscattered electrons from both layers are detectable by SEM, these bilayer regions give rise to the moiré patterns visible in the SEM image.

By contrast, the center and bottom rows in Figure 3 show the desired features: no terracing by OM, and a density of

micelles which increases smoothly from near zero in the left column to a high value in the right column. Extensive sets of SEM images were acquired on the 50 wt %/45K and 50 wt %/107K films (selected images from both these films are shown in Figure 3), along with a 60 wt %/45K film. The areal density of micelles is plotted against film thickness for these three films in Figure 4; in each film, the density extends from near zero up to ~ 500 micelles/ μm^2 , comparable to the areal density for neat PS/PI 62/11 (800 micelles/ μm^2).

Model for Micelle Areal Density. We can capture the quantitative relationship between micelle density and film thickness via a simple geometric model. As noted previously, a minimum film thickness t_0 is required before any micelles can form. In the neat diblock, $t_0 = b$; in the dry-brush limit, the homopolymer does not penetrate the wetting layers, but simply resides between them, increasing t_0 proportionally:

$$t_0 = \frac{b}{(1-\phi)} \quad (1)$$

where ϕ is the volume fraction of homopolymer (0.494 and 0.594 for the 50 and 60 wt % homopolymer blends, respectively, using polymer mass densities²³ of 1.05 and 0.90 g/cm³ for PS and PI). For $t > t_0$, micelles can form at an areal density n , which is related to the areal density in the neat diblock n_0 as

$$n = \left(\frac{t-t_0}{m} \right) (1-\phi) n_0 \quad (2)$$

Together, the proportionality constants within parentheses in eq 2 simply represent the effective thickness of block copolymer contained in the “extra” thickness of film, $(t - t_0)(1 - \phi)$, divided by the thickness of block copolymer (m) required to form each layer of spheres in a film of the neat block copolymer. Like eq 1, eq 2 also corresponds to the dry-brush limit, if m and n_0 are taken to be the values for the neat diblock; in the dry-brush limit, the homopolymer does not penetrate the micelle corona, so the micelle size is unchanged from the neat case. As noted above, $m = (2/3)^{1/2}a$, and for a

hexagonal lattice, $n_0 = (2/\sqrt{3})/a^2$, so eq 2 may be rewritten as:

$$n = \left(\frac{\sqrt{2}(1-\varphi)}{a^3} \right) (t - t_0) \quad (3)$$

Equations 1 and 3 define the anticipated shape of the n vs t curve for which data are shown in Figure 4: $n = 0$ for $t \leq t_0$, and a straight line with slope $\sqrt{2}(1-\varphi)/a^3$ for $t \geq t_0$. There is no upper thickness limit to the validity of eq 3, though it is important to recognize that all micelles do not lie at precisely the same vertical position within the film; the structure becomes increasingly “three-dimensional” as the film thickness is increased. Consequently, in films which have thicknesses greater than the average intermicelle distance, the projections of the micelles onto the substrate will begin to overlap, making such thick films useless for pattern transfer,⁶ since well-separated dots are generally desired. Consequently, we confine ourselves to film thicknesses for which $n \approx 0.7n_0$ or less. The solid black line in Figure 4 corresponds to the prediction of eqs 1 and 3 for $\varphi = 0.494$, using $a = 38$ nm and $b = 38$ nm, as measured independently for the neat PS/PI 62/11. The agreement with the data for the 50 wt %/107K film is excellent, confirming that this blend system is in the dry-brush limit, and validating the simple model presented above.

When the homopolymer molecular weight is reduced, some penetration of the wetting layers by the homopolymer will occur, reducing t_0 from the value given in eq 1. Similarly, penetration of the micelle coronae by homopolymer increases the curvature of the micelle core, reducing the micelle size and increasing the micelle number density.²⁴ Both of these effects (reduced x -intercept, increased slope) are evident in Figure 4, when the data for the 50 wt %/45K film are compared with those for the 50 wt %/107K film. For the former blend, the ratio of homopolymer to corona block M_n is 0.73, so some interpenetration is expected. While the degree of interpenetration is difficult to assess independently, it can be accounted for in the model by reducing both b (in eq 1) and a (in eq 3) from their values for neat PS/PI 62/11, to capture the effects of interpenetration. The dashed red curve (for $\varphi = 0.494$) and dotted blue curve (for $\varphi = 0.594$) are calculated with $b = 37$ nm (3% less than for neat PS/PI 62/11), and $a = 33$ nm (13% less than for neat PS/PI 62/11). A good description of the two 45K homopolymer data sets (50 and 60 wt %) is obtained with this common set of b and a values. Somewhat greater interpenetration of the micelle coronae than of the wetting layers is expected, since the micelles have the “natural” curvature for an asymmetric diblock, while in the wetting layers, the block copolymer chains are forced into a lamellar geometry in which the majority block is even more stretched than it is in the micelles. While the limited contrast and resolution in the SEM images prevents direct measurements of micelle size with the necessary precision, a 13% reduction in a implies the same fractional reduction in the micelle diameter.

In conclusion, we have demonstrated the ability to create polymer thin films that possess custom-tailored areal densities of micelles, simply by controlling the film thickness at a fixed and moderate homopolymer content. A simple geometric model in the dry-brush limit allows prediction of the film thickness required to achieve a desired micelle density,

knowing only the structural parameters (wetting layer thickness and intersphere spacing) determined independently on the neat block copolymer. Further work will explore the use of these low-density micelle arrays as templates for nanofabrication.

Acknowledgment. The authors wish to thank Bryan Beckingham (Princeton) for characterization of the polymers used and Dan Angelescu (Princeton) for construction of the original version of the flow coater. This project was generously supported by the Xerox Foundation, and by the National Science Foundation MRSEC Program through the Princeton Center for Complex Materials (DMR-0819860).

Supporting Information Available: Text containing the polymer molecular weight characterization, description of the flow-coating method used to prepare thickness-gradient films, and film characterization methods, including the image analysis protocol, and a figure showing the representative image analysis results. This material is available free of charge via the Internet at <http://pubs.acs.org>.

References and Notes

- (1) Bates, F. S.; Fredrickson, G. H. *Annu. Rev. Phys. Chem.* **1990**, *41*, 525–557.
- (2) Hamley, I. W. *The Physics of Block Copolymers*; Oxford University Press: Oxford, U.K., 1998.
- (3) Hamley, I. W. *Prog. Polym. Sci.* **2009**, *34*, 1161–1210.
- (4) Marencic, A. P.; Register, R. A. *Annu. Rev. Chem. Biomol. Eng.* **2010**, *1*, 277–297.
- (5) Park, M.; Chaikin, P. M.; Register, R. A.; Adamson, D. H. *Appl. Phys. Lett.* **2001**, *79*, 257–259.
- (6) Vedrine, J.; Hong, Y. R.; Marencic, A. P.; Register, R. A.; Adamson, D. H.; Chaikin, P. M. *Appl. Phys. Lett.* **2007**, *91*, 143110.
- (7) Cheng, J. Y.; Ross, C. A.; Chan, V. Z. H.; Thomas, E. L.; Lammertink, R. G. H.; Vancso, G. J. *Adv. Mater.* **2001**, *13*, 1174–1178.
- (8) Naito, K.; Hieda, H.; Sakurai, M.; Kamata, Y.; Asakawa, K. *IEEE Trans. Magn.* **2002**, *38*, 1949–1951.
- (9) Jung, Y. S.; Ross, C. A. *Small* **2009**, *5*, 1654–1659.
- (10) Li, R. R.; Dapkus, P. D.; Thompson, M. E.; Jeong, W. G.; Harrison, C.; Chaikin, P. M.; Register, R. A.; Adamson, D. H. *Appl. Phys. Lett.* **2000**, *76*, 1689–1691.
- (11) Yoshida, S.; Ono, T.; Esashi, M. *Nanotechnology* **2008**, *19*, 475302.
- (12) Hays, D. A.; Bolte, S. B.; Zona, M. F.; Kubby, J. A. U.S. Patent 7,228,091, issued June 5, 2007 to Xerox Corporation.
- (13) Hu, J. T.; Odom, T. W.; Lieber, C. M. *Acc. Chem. Res.* **1999**, *32*, 435–445.
- (14) Harrison, C.; Park, M.; Chaikin, P. M.; Register, R. A.; Adamson, D. H.; Yao, N. *Polymer* **1998**, *39*, 2733–2744.
- (15) Oh, H.; Green, P. F. *Macromolecules* **2008**, *41*, 2561–2566.
- (16) Smith, A. P.; Douglas, J. F.; Meredith, J. C.; Amis, E. J.; Karim, A. *Phys. Rev. Lett.* **2001**, *87*, 015503.
- (17) Mishra, V.; Hur, S. M.; Cochran, E. W.; Stein, G. E.; Fredrickson, G. H.; Kramer, E. J. *Macromolecules* **2010**, *43*, 1942–1949.
- (18) Winey, K. I.; Thomas, E. L.; Fetters, L. J. *Macromolecules* **1992**, *25*, 2645–2650.
- (19) Shull, K. R.; Winey, K. I. *Macromolecules* **1992**, *25*, 2637–2644.
- (20) Hasegawa, H.; Hashimoto, T. *Polymer* **1992**, *33*, 475–487.
- (21) Stafford, C. M.; Roskov, K. E.; Epps, T. H., III; Fasolka, M. J. *Rev. Sci. Instrum.* **2006**, *77*, 023908.
- (22) Crocker, J. C.; Grier, D. G. *J. Colloid Interface Sci.* **1996**, *179*, 298–310.
- (23) Khandpur, A. K.; Forster, S.; Bates, F. S.; Hamley, I. W.; Ryan, A. J.; Bras, W.; Almdal, K.; Mortensen, K. *Macromolecules* **1995**, *28*, 8796–8806.
- (24) Kinning, D. J.; Thomas, E. L.; Fetters, L. J. *Macromolecules* **1991**, *24*, 3893–3900.